Evanescent-Field Optical Readout of Graphene Mechanical Motion at Room Temperature

Robin M. Cole, George A. Brawley, Vivekananda P. Adiga, Roberto De Alba, Jeevak M. Parpia, Bojan Ilic, Harold G. Craighead, and Warwick P. Bowen

Evanescent field optical readout of graphene mechanical motion at room temperature

Robin M. Cole,[1] George A. Brawley,[1] Vivekananda P. Adiga,[2] Roberto De Alba,[3]
Jeevak M. Parpia,[3] Bojan Ilic,[4] Harold G. Craighead,[2] and Warwick P. Bowen[1]

[1]*Queensland Quantum Optics Laboratory, University of Queensland Brisbane, QLD 4072, Australia.*
[2]*School of Applied and Engineering Physics, Cornell University, 205 Clark Hall, Ithaca, New York 14853, USA.*
[3]*Department of Physics, Cornell University, 109 Clark Hall, Ithaca, New York 14853, USA.*
[4]*Cornell Nanoscale Science and Technology Facility,*
Cornell University, 250J Duffield Hall, Ithaca, New York 14853, USA.

Graphene mechanical resonators have recently attracted considerable attention for use in precision force and mass sensing applications. To date, readout of their oscillatory motion has typically required cryogenic conditions to achieve high sensitivity, restricting their range of applications. Here we report the first demonstration of evanescent optical readout of graphene motion, using a scheme which does not require cryogenic conditions and exhibits enhanced sensitivity and bandwidth at room temperature. We utilize a high Q microsphere to enable evanescent readout of a 70 μm diameter graphene drum resonator with a signal-to-noise ratio of greater than 25 dB, corresponding to a transduction sensitivity of $S_N^{1/2} = 2.6 \times 10^{-13}$ m Hz$^{-1/2}$. The sensitivity of force measurements using this resonator is limited by the thermal noise driving the resonator, corresponding to a force sensitivity of $F_{min} = 1.5 \times 10^{-16}$ N Hz$^{-1/2}$ with a bandwidth of 35 kHz at room temperature (T = 300 K). Measurements on a 30 μm graphene drum had sufficient sensitivity to resolve the lowest three thermally driven mechanical resonances. The graphene drums coupled both dispersively and dissipatively to the optical field with coupling coefficients of $G/2\pi = 0.21$ MHz/nm and $\Gamma_{dp}/2\pi = 0.1$ MHz/nm, respectively.
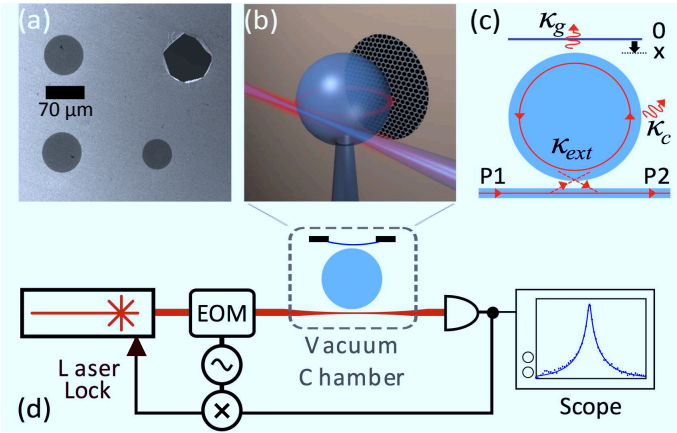
FIG. 1. (a) SEM image of a graphene drum resonator's, a broken drum shows the contrast due to the graphene. (b) Illustration showing a microsphere with a graphene resonator in the evanescent field. (c) Illustration showing the optical coupling rates associated with the cavity measurement, discussed in the text. (d) Schematic of the measurement system.

I. INTRODUCTION

Micro and nano-electro-mechanical (NEMS) force sensors are broadly applied in accelerometry[1], magnetometry[2], thermometry[3], navigation[4], geodesy[5], medical diagnosis[6], and have a range of specialized applications in areas such as atomic force microscopy[7], nanoscale spin-resonance imaging [8], and quantum information science[9]. Currently silicon is the material of choice for fabricating precision NEMS force

sensors, enabling the production of devices with both high sensitivity and large bandwidths[10, 11]. However graphene resonators have excellent mechanical properties and exceptionally low mass per unit area[12–14], which makes them attractive candidates for use in ultrasensitive force[15–18] and mass[19–22] measurements, as well as for quantum optomechanics[23–26].

In a generic NEMS force sensor, the motion of a compliant mechanical resonator is tracked optically or electrically as it responds to external forces[27]. To reduce the measurement noise and enhance the measurement bandwidth a new approach has been developed where an optical or microwave cavity is used to control and readout the motion of the resonator[28, 29]. These cavity optomechanical systems allow force sensitivity at the fundamental thermomechanical noise floor $F_{min} = \sqrt{4 m_{\text{eff}} \Gamma_m k_B \text{T}}$ in N Hz$^{-1/2}$ where m_{eff} is the effective mass of the mechanical resonator, Γ_m its mechanical dissipation rate, k_B is the Boltzmann constant and T its temperature. Here we place graphene resonators into a cavity optomechanical system and demonstrate the sensitive readout of their motion at room temperatures, thus paving the way for the more widespread application of graphene NEMS force sensors.

Outside of the field of optomechanics, over the past 10 years much progress has been made in the experimental characterization of the unique material properties of graphene, including large thermal[30] and electrical[12] conductivity, record breaking Young's modulus[31], length-dependent thermal conductivity[32] and broadband constant $\pi\alpha = 2.3\%$ optical absorption[33], among others. However, to date measurements have been performed on graphite or graphene that is in contact with a substrate, or else on suspended sheets that are electri-

cally actuated or contacted in ways that influence their measurement. For instance, measurements on the size dependent[13] and non-linear dissipation[34] of graphene membranes are currently convoluted with the influence of the applied gate voltage required to drive and detect their motion. Our results provide a new approach to study these material properties on micron-scale graphene films in thermal equilibrium at room temperature.

Graphene's large electrical conductivity[35] and relatively straightforward integration into circuits has enabled sensitive motion readout using microwave electromechanical measurement systems[16]. In these systems, both static (DC) and time-varying (RF) forces can be applied to the resonator, allowing tuning of the resonance frequency (through static deflection of the resonator) and the study of driven non-linearities[23–25, 36]. However this approach requires cryogenic cooling of the electrical amplifiers owing to the relatively high Johnson (electrical) noise floor which severely limits the range of potential applications. Overcoming this requirement, measurement systems utilizing visible optical wavelengths have been demonstrated at room temperatures [16, 37, 38]. The alternative approach described here uses near-field evanescent sensing[29, 39]. The graphene resonator is placed in the evanescent field of a high Q silica microsphere, with the motion of the graphene imparted onto the phase of the optical field circulating within the cavity. Crucially, in this arrangement the signal due to the graphene resonator is enhanced by the high optical Q factor and the steep gradient of the evanescent field, lifting the signal above of the noise floor and enabling motion readout with large SNR[40]. An interesting feature of graphene mechanical resonators is that they couple both dispersively and dissipatively to the optical field, in contrast to the majority of other resonators which are purely dispersively coupled[39]. Dissipative coupling enables enhanced optical transduction[41], and could be utilised in novel dissipative optomechanics systems[42–45].

II. METHODOLOGY

A. Experimental setup

An SEM image showing graphene circular drum resonator's studied in this work is shown in Fig.1(a). The graphene is produced by chemical vapor deposition (CVD) on a copper foil and transferred to a silicon substrate[13] with pre-patterned circular through holes. Measurements have been performed on resonators with diameters in the range of d = 20 to 70 μm that support fundamental mechanical resonances in the range of $\omega_m/2\pi \approx 1$ to 5 MHz[13, 46]. An illustration of the motion readout measurement is shown in Fig.1(b). A graphene resonator is shown placed within the evanescent field of a microsphere, typically at a distance of 50 - 100 nm from the microsphere surface. A tapered optical fiber is used to couple laser light to an optical res-
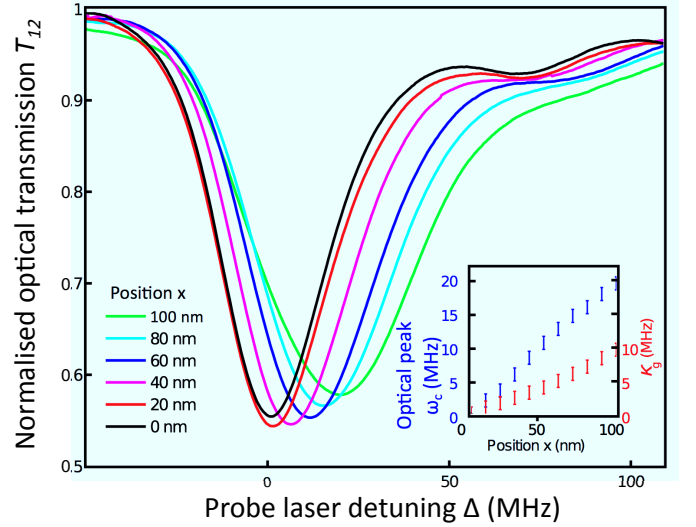

FIG. 2. Experimentally measured normalized transmission (T_{12}) spectra with position of the graphene resonator x within the evanescent field. At 0 nm the graphene is far from the microsphere surface, at 100 nm it is almost touching. Laser detuning is defined as $\Delta = 0$ at ω_c for the $x = 0$ nm spectra. (inset) Extracted optical resonance frequency ω_c and loss due to the graphene κ_g.

onance of the microsphere[47]. The taper and the chip containing the graphene drums are mounted on separate three axis nano-positioning stages and aligned around the fixed microsphere. This system is housed within a custom built vacuum chamber that is maintained at a pressure of 3×10^{-7} Torr using a vibration free ion pump. Compared with monolithic systems where the optical and mechanical resonators are fabricated upon a single chip[10, 29], this approach provides wide flexibility in the choice of optomechanic coupling strength, and places fewer constraints on the device fabrication. This comes at the cost of increased complexity in the experimental alignment and stabilization.

B. Optical characterization

Referring to the illustration in Fig.1(c), a small displacement ∂x of the graphene resonator produces both a dispersive and a dissipative modification to the optical resonance. Focusing first on the dispersive effect, the displacement shifts the resonance by an amount $\partial \omega_c$, where the magnitude of this shift is determined by the optomechanical coupling coefficient G that quantifies the overlap of the optical field with the graphene resonator, such that $G = \partial \omega_c / \partial x$. The dissipative effect increases the optical linewidth (full width at half maximum) $\kappa = \kappa_c + \kappa_g + \kappa_{ext}$ where κ_c is the internal cavity loss rate due to the intrinsic losses of the cavity (e.g. due to surface roughness), κ_{ext} is the external coupling rate between the taper and optical resonance, and κ_g is the optical loss due

to the graphene (i.e. due to its 2.3% absorption). By analogy to the dispersive coupling coefficient, we can define a dissipative optomechanical coupling coefficient[41] $\Gamma_{dp} = \partial\kappa/\partial x$. The sensitivity of motion measurements depends on the values of G and Γ_{dp}, which depend on the particular mechanical and optical resonators under measurement. Here we show that despite the optical loss introduced by the graphene, motion readout measurements with high sensitivity are possible using cavity enhanced evanescent sensing.

III. RESULTS AND DISCUSSION

A. Optical coupling coefficients

The measurement system is shown in Fig.1(d). To characterize G and Γ_{dp} a 780 nm diode laser outputting power P1 is swept over an optical resonance of the microsphere and the transmitted optical power P2 is recorded as a function of the position x of the graphene within the evanescent field. The absolute distance between the graphene drum and microsphere was calibrated by offsetting the drum laterally, bringing the Si substrate into contact with the microsphere, and recording the stage readings. Fig.2 shows spectra of the normalized optical transmission $T_{12} = $ P2/P1. These measurements were performed with a 70 μm diameter graphene resonator and a 60 μm diameter microsphere. Both ω_c and κ are modified by the presence of the graphene. The spectra are described by[48] $T_{12} = \frac{(\kappa_c + \kappa_g - \kappa_{ext})^2 + 4\Delta^2}{(\kappa_c + \kappa_g + \kappa_{ext})^2 + 4\Delta^2}$, where $\Delta = \omega_p - \omega_c$ is the detuning of the incident laser pump ω_p from the optical resonance ω_c. Here we assume that since κ_c is a fixed property of the optical resonance, increases in κ are due to the optical loss introduced by the graphene κ_g. The extracted values of κ_g with position x are shown in the inset of Fig.2. Extraction of κ_g allows calculation of the optical power dissipated by the graphene, discussed later. Whilst drift of the substrate position will cause a change in κ_{ext}, this drift was calibrated using an optical resonance and found to be small compared to the changes in κ_g over the time-scale of these measurements. A fit to a spectra recorded without the graphene present gave the intrinsic cavity loss rate $\kappa_c/2\pi$ = 10.2 MHz, corresponding to an optical quality factor $Q = \omega_c/\kappa_c = 3 \times 10^7$. Fitting spectra to $\partial\omega_c = G\partial x$ and $\partial\kappa = \Gamma_{dp}\partial x$ yields both dispersive $G/2\pi = 0.21$ MHz/nm and dissipative $\Gamma_{dp}/2\pi = 0.1$ MHz/nm coupling coefficients. Many dissipative optomechanics applications[42–45] require that dissipative coupling is maximized and dispersive coupling minimized. Here we achieve G/Γ_{dp} = 2.1 which compares favorably to a value of $G/\Gamma_{dp} = 4$ recently reported for a cavity torque sensor[41].

It is important to note that the values of G and Γ_{dp} reported here overestimate the coupling that can be achieved in practical transduction measurements since they do not take into account the mechanical mode shape, but approximate the motion as a uniform shift of the resonator into the optical mode. From carefully calibrated measurements of the thermal amplitude of the mechanical resonance it is possible to determine the true dynamical coupling rates G_{dy} for each optical and mechanical mode pair, as reported elsewhere for silicon nanostrings[39]. However, in the limit of a point-like measurement of the fundamental mode, the value of G reported here converges with the dynamic coupling rate. Our measurements are close to point-like where here the transverse optical sampling length $l_y \approx 10\mu m$ is short compared to the graphene drum diameter. A simple calculation based on the mean displacement of the mechanical mode within the optical sampling length indicates that for our measurements $G_{dy}/G = 0.99$, assuming perfect alignment of the optical mode with the mechanical mode. In practice, the alignment is performed by eye using a microscope system, and is estimated to be accurate to +/- 5μm, placing a lower bound on the coupling rate of $G_{dy}/G = 0.96$.

B. Motion transduction

To demonstrate the use of graphene resonators as sensitive force sensors we present experimental data showing the motion readout of the mean-square displacement $\langle x(t)^2 \rangle$ of the resonator arising from the random thermal (Brownian) force fluctuations F_T driving the resonator. These fluctuations are distributed in frequency ω according to $x(\omega) = F_T\chi_m(\omega)$ where the resonator's Lorentzian-shaped susceptibility $\chi_m(\omega) = [m_{\text{eff}}(\omega_m^2 - \omega^2 - i\Gamma_m\omega)]^{-1}$, and F_T is modeled as a white-noise. The power-spectral-density (PSD) of the random displacements of the resonator is given by $S_{xx}(\omega) = 4m_{\text{eff}}\Gamma_m k_B T|\chi_m^2(\omega)|$[49]. The optomechanical coupling G transduces the motion of the resonator into frequency noise on the optical resonance via $G = \sqrt{S_{\omega\omega}/S_{xx}}$. The measured signal is given by $S = S_{\omega\omega} + S_N$ where S_N is the measurement noise (e.g. due to detector noise). At $\omega = \omega_m$ the measurement SNR $= \frac{S_{\omega\omega}}{S_N} = \frac{4k_B T}{m_{\text{eff}}\Gamma_m\omega_m^2 S_N}$, which on rearranging gives the noise limited measurement uncertainty

$$S_N^{1/2} = \left[\frac{4k_B T}{m_{\text{eff}}\Gamma_m\omega_m^2 \text{SNR}}\right]^{1/2} \qquad (1)$$

Readout of graphene motion is performed using the system shown in Fig 1(d). The taper and graphene resonator are mounted on nano-positioning stages and aligned around the microsphere. To ensure high mechanical Q, the measurement is performed within a vacuum chamber that is maintained at a pressure of 3×10^{-7} Torr using a vibration free ion pump. The output from the laser is fibre coupled and passes through an electro-optic modulator (EOM) which applies a 100 MHz phase modulation to produce the error signal for the Pound-Drever-Hall (PDH) laser lock. The laser is locked to
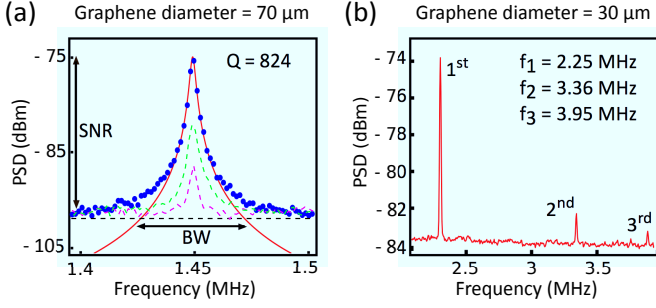
FIG. 3. (a) Measured spectrum showing the fundamental mechanical resonance of a 70 μm diameter graphene drum, spectrum analyzer resolution bandwidth (RBW) = 100 Hz. The traces correspond to drum displacements of - 30 nm (purple), - 15 nm (green), and 0 nm (blue) from the final position which gave maximum signal transduction. (b) Spectra showing the three lowest order resonances of a 30 μm diameter resonator, RBW = 10 kHz.

the side of the optical resonance with a fixed detuning of $\Delta = \kappa/2$, ensuring maximum transduction sensitivity. The T_{12} transmitted light is incident on a low-noise photodetector, and monitored using an oscilloscope and a spectrum analyser. The measured mechanical spectra for a diameter d = 70 μm resonator is shown in Fig.3(a). The resonator was placed within the evanescent field and transduction spectra recorded at three positions along the field gradient. The relative displacement between measurement positions was read out using the nano-positioning stage control software, but the absolute displacement between the graphene and sphere was not precisely known. The traces correspond to displacements of - 30 nm (purple dashed trace), - 15 nm (green trace), and 0 nm (blue dots) where the final position gave maximum signal transduction. The increasing gradient of the optical field means that transduction sensitivity is greatest for the smallest displacement between the graphene and sphere. However, as the graphene approaches the surface of the sphere the risk of contact, and subsequent destruction of the drum increases. The observed mechanical resonance is fit to a Lorentzian lineshape (red line) with the fit to the white-noise background indicated by the black dashed line. The mechanical resonance peak rises 25 dB above the flat measurement background, defining the measurement SNR. Assuming a pristine monolayer graphene the effective mass of the fundamental drum mode of the resonator is calculated from[24] $m_{\mathrm{eff}} = 0.27\pi r^2 \rho_{2D} = 7.9 \times 10^{-16}$kg where the mass density $\rho_{2D} = 7.9 \times 10^{-19}$ kg /μm^2 and r = d/2. From the Lorentzian fit, $\omega_m/2\pi = 1.44$ MHz and $\Gamma_m/2\pi = 1.75$ kHz. Substituting these values into Eq.1 yields the transduction sensitivity of $S_N^{1/2} = 2.6 \times 10^{-13}$ m Hz$^{-1/2}$, which is currently limited by the Q factor of the microsphere. As a force sensor this graphene resonator would enable measurements with a force sensitivity of $F_{min} = 1.5 \times 10^{-16}$ N Hz$^{-1/2}$ at room temperature

(T = 300 K). The usable bandwidth in this scenario is given by the frequency range for which the mechanical resonance is resolved with a SNR > 1, marked in Fig.3(a). For this resonator the force measurement bandwidth = 35 kHz. For comparison, the authors of measurements using a low-Finesse cavity[38] report a position sensitivity of $S_N^{1/2} = 6 \times 10^{-13}$ m Hz$^{-1/2}$ for an optically cooled resonator, where the measurement is intrinsically limited by photodetector noise.

Referring to Fig.3(b), measurements on a 30 μm diameter resonator have sufficient SNR to resolve the 1st, 2nd and 3rd mechanical resonances in the thermal noise driven motion with frequencies of $\omega_m/2\pi = 2.25$, 3.36 and 3.95 MHz and Q factors of 528, 884 and 927 respectively. The frequencies of these modes match reasonably well to previous measurements and the predictions of a simple model for the resonant frequency of circular drum resonances, expected at 1.59 and 2.14 times the fundamental frequency[38]. The ability to resolve multiple mechanical modes is potentially useful for mass sensing[50] and for characterizing the non-linear mechanical properties of the resonators[51].

C. Parametric tuning

For applications it is desirable to be able to rapidly tune the mechanical frequency of the graphene resonator, for example to enable force sensing at specific frequency bands, or to generate parametric non-linearities which enable the detection of weak signals within measurement noise[52]. Here we demonstrate this via the photothermal tension (σ_{pth}) induced in the membrane by optical absorption. Motion readout spectra in Fig.4 shows the tuning of the mechanical resonance ω_m as a function of optical power dissipated by the graphene P_g. Powers P1 in the range 5 to 30μW produced tuning over a range of 20 kHz. No change in the mechanical decay rate was observed. We define the effective mechanical frequency as $\omega_{\mathrm{eff}} \approx \omega_m \left(1 + \frac{\sigma_{pth}}{2\sigma_0}\right)$ which is valid in the limit $\sigma_{pth} \ll \sigma_0$, where σ_0 is the intrinsic tension in the resonator membrane. According to theory[38], photons absorbed by the graphene induce a tension in the resonator membrane $\sigma_{pth} = AP_g$ where A is a material constant which depends on the absorption, thermal conductivity and thermal expansion coefficients of graphene. Fitting[48] $P_g/P1 = \left(\frac{4\kappa_{ext}\kappa_g}{\kappa^2 + 4\Delta^2}\right)$, yields P_g used in the inset plot of Fig.4. From a linear fit to ω_{eff} v.s P_g a value of $A = 9.3$ N/(m W) is extracted, which is in reasonable agreement with a value of $A = 15$ N/(m W) calculated using the fundamental constants of graphene[38]. In principle a significantly wider tuning range can be achieved by increasing the in-taper optical power P1. For example, a readily achievable P1 of 3 mW would increase the tuning range to 2 MHz; while incident powers as high as 400 mW have been reported recently[53]. The bandwidth of photothermal parametric control, achieved for example
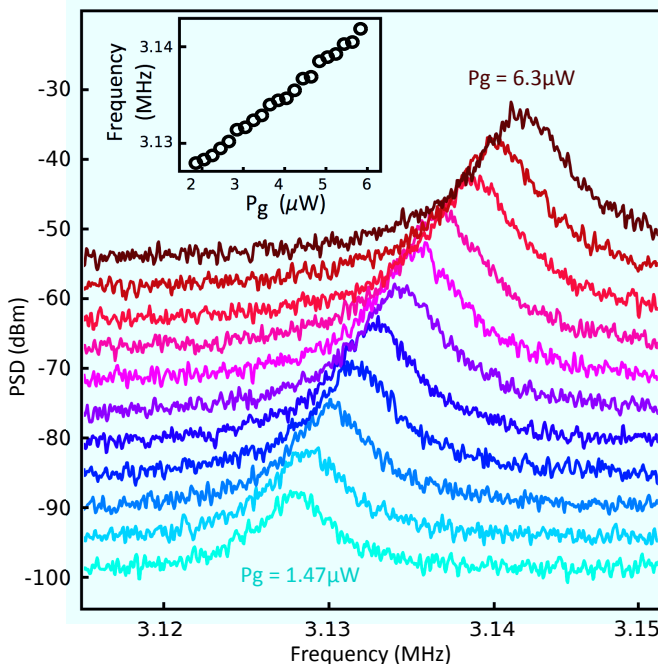
FIG. 4. Mechanical resonance spectra of a 20 μm diameter resonator with optical power dissipated by the graphene P_g, with (inset) extracted resonance peak ω_{eff}. Spectra offset by 2.5 dBm on the vertical scale.

using amplitude modulated light, is limited by the thermalisation time τ of the graphene drum. For a circular membrane[38] $\tau = a^2 \rho C / 2\kappa$, where a is the membrane radius, $C = 700$ J/(kgK) is the specific heat of graphene, $\kappa = 5000$ W/(m K) is the thermal conductivity[54], and $\rho = 2200$ kg/m^3 the density. Taking $a = 10$ μm yields the thermalization time $\tau = 15.4$ ns, corresponding to response bandwidth of ≈ 65 MHz. This rate is sufficient to generate the parametric non-linearities described in [52]. Finally dissipation of P_g causes an increase in temperature T of the resonator $\Delta T = \beta P_g$ where the constant of proportionality $\beta = (2\pi t k)^{-1}$ and $t = 0.335$ nm the thickness of a monolayer. The maximum value of $P_g = 6.3\mu W$ gives $\Delta T = 0.59$ K, which is a small change relative to room temperature (300 K). Therefore we conclude that for moderate optical powers heating will not significantly degrade the sensitivity F_{min} of force measurements using this resonator.

IV. OUTLOOK AND CONCLUSION

State of the art silicon cantilevers achieve a force sensitivity of $F_{min} = 5.3 \times 10^{-17}$ N Hz$^{-1/2}$ at room temperature[11], owing to their high mechanical Q factors. However, their relatively large mass places an intrinsic limit on their sensitivity. In contrast, improved high Q factor graphene resonators would constitute ultra-sensitive force sensors with exceptionally small physical dimensions. The optomechanical coupling and hence measurement bandwidth scales as[39] $G \propto (V_{nano}/V_{cav})$ where V_{nano} is the volume of the mechanical oscillator sampled by the optical cavity with mode volume V_{cav}. The microspheres used in this work are of relatively large diameters, and the optical resonances selected were not low-order modes. Therefore careful optimization of the ratio V_{nano}/V_{cav} could yield significant improvement in G. Furthermore, by switching to homodyne detection an improvement in readout sensitivity is readily attainable, and would allow the direct measurement of the vacuum optomechanical coupling rate using frequency noise calibration[55]. Finally, appropriate band-gap engineering of the graphene could further mitigate the negative effects of optical absorption.

In conclusion, we have demonstrated the readout of graphene NEMS motion at room temperature using cavity enhanced evanescent sensing with high Q optical microspheres. This approach enables ultra-sensitive readout of the graphene oscilliatory motion, and paves the way for high sensitivity/large bandwidth room temperature force measurements in a resonator mass regime not currently attainable using silicon NEMS devices. We present the first measurement of the *dispersive and dissipative* optomechanical coupling coefficients of graphene at visible wavelengths, and show that material absorption does not result in poor readout sensitivity, and only minimally heats the resonator. Finally, we exploit the optical absorption to tune the mechanical frequency of the graphene resonator, and propose routes to improving the sensitivity of readout measurements.

V. ACKNOWLEDGMENTS

[1] A. G. Krause, M. Winger, T. D. Blasius, Q. Lin, and O. Painter, "A high-resolution microchip optomechanical accelerometer," Nature Photonics **6**, 768 (2012).

[2] S. Forstner, E. Sheridan, J. Knittel, C. Humphreys, G. Brawley, H. Rubinsztein-Dunlop, and W. Bowen, "Ultrasensitive Optomechanical Magnetometry," Advanced materials **26**, 6348 (2014).

[3] G. I. Harris, D. L. McAuslan, T. M. Stace, A. C. Doherty, and W. P. Bowen, "Minimum Requirements for Feedback Enhanced Force Sensing," Physical Review Letters **111**, 103603 (2013).

[4] G. Krishnan, C. U. Kshirsagar, G. K. Ananthasuresh, and N. Bhat, "Micromachined high-resolution accelerometers," Journal of the Indian Institute of Science **87**, 333 (2012).

[5] N. Yazdi, F. Ayazi, and K. Najafi, "Micromachined inertial sensors," Proceedings of the IEEE **86**, 1640 (1998).

[6] N. Maluf, D. Gee, K. Petersen, and G. Kovacs, "Medical applications of MEMS," in *Proceedings of WESCON'95* (IEEE, 1995) p. 300.

[7] K. Srinivasan, H. Miao, M. T. Rakher, M. Davanço, and V. Aksyuk, "Optomechanical transduction of an integrated silicon cantilever probe using a microdisk resonator." Nano letters **11**, 791 (2011).

[8] D. Rugar, R. Budakian, H. J. Mamin, and B. W. Chui, "Single spin detection by magnetic resonance force microscopy." Nature **430**, 329 (2004).

[9] M. D. LaHaye, J. Suh, P. M. Echternach, K. C. Schwab, and M. L. Roukes, "Nanomechanical measurements of a superconducting qubit." Nature **459**, 960 (2009).

[10] C. Doolin, P. H. Kim, B. D. Hauer, a. J. R. MacDonald, and J. P. Davis, "Multidimensional optomechanical cantilevers for high-frequency force sensing," New Journal of Physics **16**, 035001 (2014).

[11] H. Miao, K. Srinivasan, and V. Aksyuk, "A microelectromechanically controlled cavity optomechanical sensing system," New Journal of Physics **14**, 075015 (2012).

[12] A. Geim and K. Novoselov, "The rise of graphene." Nature materials **6**, 183 (2007).

[13] R. A. Barton, B. Ilic, A. M. van der Zande, W. S. Whitney, P. L. McEuen, J. M. Parpia, and H. G. Craighead, "High, size-dependent quality factor in an array of graphene mechanical resonators." Nano letters **11**, 1232 (2011).

[14] A. K. Hüttel, G. A. Steele, B. Witkamp, M. Poot, L. P. Kouwenhoven, and H. S. van der Zant, "Carbon nanotubes as ultrahigh quality factor mechanical resonators." Nano letters **9**, 2547 (2009).

[15] A. Eichler, J. Moser, J. Chaste, M. Zdrojek, I. Wilson-Rae, and A. Bachtold, "Nonlinear damping in mechanical resonators made from carbon nanotubes and graphene." Nature nanotechnology **6**, 339 (2011).

[16] J. S. Bunch, A. M. van der Zande, S. S. Verbridge, I. W. Frank, D. M. Tanenbaum, J. M. Parpia, H. G. Craighead, and P. L. McEuen, "Electromechanical resonators from graphene sheets." Science (New York, N.Y.) **315**, 490 (2007).

[17] J. Moser, J. Güttinger, A. Eichler, M. J. Esplandiu, D. E. Liu, M. I. Dykman, and A. Bachtold, "Ultrasensitive force detection with a nanotube mechanical resonator." Nature nanotechnology **8**, 493 (2013).

[18] S. Stapfner, L. Ost, D. Hunger, J. Reichel, I. Favero, and E. M. Weig, "Cavity-enhanced optical detection of carbon nanotube Brownian motion," Applied Physics Letters **102**, 151910 (2013), arXiv:arXiv:1211.1608v1.

[19] J. Chaste, A. Eichler, J. Moser, G. Ceballos, R. Rurali, and A. Bachtold, "A nanomechanical mass sensor with yoctogram resolution." Nature nanotechnology **7**, 301 (2012).

[20] K. Jensen, K. Kim, and A. Zettl, "An atomic-resolution nanomechanical mass sensor." Nature nanotechnology **3**, 533 (2008).

[21] H.-Y. Chiu, P. Hung, H. W. C. Postma, and M. Bockrath, "Atomic-scale mass sensing using carbon nanotube resonators." Nano letters **8**, 4342 (2008).

[22] Y. T. Yang, C. Callegari, X. L. Feng, K. L. Ekinci, and M. L. Roukes, "Zeptogram-scale nanomechanical mass sensing." Nano letters **6**, 583 (2006).

[23] X. Song, M. Oksanen, J. Li, P. Hakonen, and M. Sillanpää, "Graphene Optomechanics Realized at Microwave Frequencies," Physical Review Letters **113**, 027404 (2014).

[24] P. Weber, J. Güttinger, I. Tsioutsios, D. E. Chang, and A. Bachtold, "Coupling graphene mechanical resonators to superconducting microwave cavities." Nano letters **14**, 2854 (2014).

[25] V. Singh, S. J. Bosman, B. H. Schneider, Y. M. Blanter, A. Castellanos-Gomez, and G. a. Steele, "Optomechanical coupling between a multilayer graphene mechanical resonator and a superconducting microwave cavity." Nature nanotechnology **9**, 1 (2014).

[26] Y.-f. Shen, Y.-c. Liu, M.-y. Yan, and Y.-f. Xiao, "Dissipative optomechanics of a single-layer graphene in a microcavity," arXiv preprint arXiv: ... , 1 (2014), arXiv:1411.2202v2.

[27] K. L. Ekinci and M. L. Roukes, "Nanoelectromechanical systems," Review of Scientific Instruments **76**, 061101 (2005).

[28] F. Marquardt and S. Girvin, "Optomechanics," Physics **2**, 40 (2009).

[29] E. Gavartin, P. Verlot, and T. J. Kippenberg, "A hybrid on-chip optomechanical transducer for ultrasensitive force measurements." Nature nanotechnology **7**, 509 (2012).

[30] A. A. Balandin, S. Ghosh, W. Bao, I. Calizo, D. Teweldebrhan, F. Miao, and C. N. Lau, "Superior thermal conductivity of single-layer graphene." Nano letters **8**, 902 (2008).

[31] C. Lee, X. Wei, J. W. Kysar, and J. Hone, "Measurement of the elastic properties and intrinsic strength of monolayer graphene." Science (New York, N.Y.) **321**, 385 (2008).

[32] X. Xu, L. F. C. Pereira, Y. Wang, J. Wu, K. Zhang, X. Zhao, S. Bae, C. Tinh Bui, R. Xie, J. T. L. Thong, B. H. Hong, K. P. Loh, D. Donadio, B. Li, and B. Özyilmaz, "Length-dependent thermal conductivity in suspended single-layer graphene." Nature communications **5**, 3689 (2014).

[33] R. R. Nair, P. Blake, A. N. Grigorenko, K. S. Novoselov, T. J. Booth, T. Stauber, N. M. R. Peres, and A. K. Geim, "Fine structure constant defines visual transparency of graphene." Science (New York, N.Y.) **320**, 1308 (2008).

[34] A. Croy, D. Midtvedt, A. Isacsson, and J. M. Kinaret, "Nonlinear damping in graphene resonators," Physical Review B **86**, 235435 (2012).

[35] A. H. Castro Neto, N. M. R. Peres, K. S. Novoselov, and A. K. Geim, "The electronic properties of graphene," Reviews of Modern Physics **81**, 109 (2009), arXiv:0709.1163.

[36] X. Song, M. Oksanen, M. a. Sillanpää, H. G. Craighead, J. M. Parpia, and P. J. Hakonen, "Stamp transferred suspended graphene mechanical resonators for radio frequency electrical readout." Nano letters **12**, 198 (2012).

[37] D. W. Carr, "Fabrication of nanoelectromechanical systems in single crystal silicon using silicon on insulator substrates and electron beam lithography," Journal of Vacuum Science & Technology B:, Microelectronics and Nanometer Structures **15**, 2760 (1997).

[38] R. A. Barton, I. R. Storch, V. P. Adiga, R. Sakakibara, B. R. Cipriany, B. Ilic, S. P. Wang, P. Ong, P. L. McEuen, J. M. Parpia, and H. G. Craighead, "Photothermal self-oscillation and laser cooling of graphene optomechanical systems." Nano letters **12**, 4681 (2012).

[39] G. Anetsberger, O. Arcizet, Q. P. Unterreithmeier, R. Rivière, A. Schliesser, E. M. Weig, J. P. Kotthaus, and T. J. Kippenberg, "Near-field cavity optomechanics with nanomechanical oscillators," Nature Physics **5**, 909 (2009).

[40] S. Forstner, J. Knittel, E. Sheridan, J. D. Swaim, H. Rubinsztein-Dunlop, and W. P. Bowen, "Sensitivity and performance of cavity optomechanical field sensors," Photonic Sensors **2**, 259 (2012).

[41] M. Wu, A. C. Hryciw, C. Healey, D. P. Lake, H. Jayakumar, M. R. Freeman, J. P. Davis, and P. E. Barclay, "Dissipative and Dispersive Optomechanics in a Nanocavity Torque Sensor," Physical Review X **4**, 021052 (2014).

[42] F. Elste, S. M. Girvin, and A. A. Clerk, "Quantum Noise Interference and Backaction Cooling in Cavity Nanomechanics," Physical Review Letters **102**, 207209 (2009).

[43] S. Huang and G. S. Agarwal, "Reactive coupling can beat the motional quantum limit of nanowaveguides coupled to a microdisk resonator," Physical Review A **82**, 033811 (2010).

[44] A. Xuereb, R. Schnabel, and K. Hammerer, "Dissipative Optomechanics in a Michelson-Sagnac Interferometer," Physical Review Letters **107**, 213604 (2011).

[45] T. Weiss and A. Nunnenkamp, "Quantum limit of laser cooling in dispersively and dissipatively coupled optomechanical systems," Physical Review A **88**, 023850 (2013).

[46] V. P. Adiga, R. De Alba, I. R. Storch, P. A. Yu, B. Ilic, R. A. Barton, S. Lee, J. Hone, P. L. McEuen, J. M. Parpia, and H. G. Craighead, "Simultaneous electrical and optical readout of graphene-coated high Q silicon nitride resonators," Applied Physics Letters **103**, 143103 (2013).

[47] J. H. Chow, M. A. Taylor, T. T.-Y. Lam, J. Knittel, J. D. Sawtell-Rickson, D. A. Shaddock, M. B. Gray, D. E. McClelland, and W. P. Bowen, "Critical coupling control of a microresonator by laser amplitude modulation." Optics express **20**, 12622 (2012).

[48] F. Monifi and J. Friedlein, "A Robust and Tunable AddDrop Filter Using Whispering Gallery Mode Microtoroid Resonator," Journal of Lightwave Technology **30**, 3306 (2012).

[49] K. L. Ekinci, "Ultimate limits to inertial mass sensing based upon nanoelectromechanical systems," Journal of Applied Physics **95**, 2682 (2004).

[50] M. S. Hanay, S. Kelber, A. K. Naik, D. Chi, S. Hentz, E. C. Bullard, E. Colinet, L. Duraffourg, and M. L. Roukes, "Single-protein nanomechanical mass spectrometry in real time." Nature nanotechnology **7**, 602 (2012).

[51] H. J. R. Westra, M. Poot, H. S. J. van der Zant, and W. J. Venstra, "Nonlinear Modal Interactions in Clamped-Clamped Mechanical Resonators," Physical Review Letters **105**, 117205 (2010).

[52] A. Szorkovszky, G. A. Brawley, A. C. Doherty, and W. P. Bowen, "Strong Thermomechanical Squeezing via Weak Measurement," Physical Review Letters **110**, 184301 (2013).

[53] J. E. Hoffman, S. Ravets, J. A. Grover, P. Solano, P. R. Kordell, J. D. Wong-Campos, L. A. Orozco, and S. L. Rolston, "Ultrahigh transmission optical nanofibers," AIP Advances **4**, 067124 (2014).

[54] A. K. Geim, "Graphene: status and prospects." Science (New York, N.Y.) **324**, 1530 (2009).

[55] M. L. Gorodetsky, A. Schliesser, G. Anetsberger, S. Deleglise, and T. J. Kippenberg, Optics express 10.1364/OE.18.023236.